Rafidain Journal of Science
https://rsci.uomosul.edu.iq
Vol. 35, No. 2, pp. 135-147, 2026 (June)

Synthesis of Activated Coke via Co-carbonization of Mixed Atmospheric Residue and Polypropylene Waste and KOH-Activation for the Desulfurization of Model Fuel

Muntaha H. Yaqoob **Abdelrahman B. Fadhil**
Department of Chemistry/College of Science/University of Mosul /Mosul/Iraq

p-ISSN: 1608-9391
e -ISSN: 2664-2786

Article information

Received: 20/ 7/ 2025
Revised: 1/ 10/ 2026
Accepted: 19/ 10/ 2025

DOI: 10.33899/rsci.v35i2.63627

Corresponding author:
Muntaha H. Yaqoob
muntaha.23scp83@student.uomosul.edu.iq
Abdelrahman B. Fadhil
abdelrahmanbasil@uomosul.edu.iq

ABSTRACT

The increasing need for environmentally friendly methods to reduce sulfur content in transportation fuels has motivated the search for efficient and low-cost adsorbents. This study aims to synthesize a novel activated coke (AC) from a combination of atmospheric residue (ATR) from the Al-Kasik refinery and polypropylene (PP) waste collected from a cement factory. The co-carbonization process was carried out at 400 °C for 1 hour, followed by chemical activation using potassium hydroxide (KOH). The resulting activated coke was characterized using X-ray diffraction (XRD), nitrogen adsorption–desorption at 77 K, field emission scanning electron microscopy (FESEM), and energy-dispersive X-ray spectroscopy (EDX) to evaluate its crystallinity, surface area, pore structure, morphology, and elemental composition. The optimized AC exhibited a surface area of 220.96 m^2/g and an average pore width of 2.95 nm, indicating a mesoporous structure. The adsorptive performance of the AC was tested using a model fuel containing dibenzothiophene (DBT) dissolved in hexane. A removal efficiency of 97.62% was achieved under optimal conditions (0.3 g of AC at 30 °C for 80 minutes). The adsorption process followed the Freundlich isotherm model and pseudo-second-order kinetics. Moreover, the AC demonstrated good reusability, retaining 88.13% removal efficiency after five regeneration cycles. The study demonstrates that the synthesized activated coke is a promising and efficient adsorbent for sulfur removal from transportation fuels, offering a sustainable solution utilizing industrial waste materials.

Keywords: Co-carbonization; Atmospheric residue; Polypropylene waste; DBT Elimination

INTRODUCTION

Liquid fuels comprise a diverse array of sulfur (S) compounds (thiophenes, thiols, sulfides, and disulfides), which are highly problematic due to their significant contribution to sulfur oxide (SOx) emissions during combustion (Suhs *et al*., 2021). Emissions of SO_x contribute to acid rain and air pollution, resulting in detrimental impacts on ecosystems and human health. Additionally, the presence of sulfur compounds in petroleum distillates can cause poisoning and deactivation of catalytic converters in vehicles, as well as induce corrosion in refinery equipment (Chen *et al*., 2021).

The oil refining industry commonly employs hydrodesulfurization (HDS) to reduce sulfur levels in transportation fuels. However, this process requires severe operating conditions—high temperatures and elevated hydrogen pressures (Moreira et al., 2017; Lv *et al*., 2022)—and remains inefficient in achieving ultra-low sulfur levels, particularly for refractory aromatic sulfur compounds such as thiophenes and their derivatives. As an alternative, adsorptive desulfurization (ADS) is considered a simple, efficient, and cost-effective technique that operates under mild conditions (Saha *et al*., 2021). It offers significant advantages, including hydrogen-free operation, low energy requirements, and the ability to selectively remove resistant sulfur compounds (Moreira *et al*., 2017). The effectiveness of this method largely depends on selecting an appropriate adsorbent with a strong affinity for aromatic sulfur species.

Various adsorbents have been studied in the ADS, including alumina, metal oxides, silica gel, carbon materials, and metal-loaded carbons (Hussein and Fadhil, 2021). Among these, activated carbon (AC) stands out for its large surface area, tunable porosity, surface functional groups, and reusability (Fadhil *et al*., 2020). AC has been prepared from numerous raw materials such as date stones (Alhamed and Bamufleh, 2009). PET waste (Fadhil *et al*., 2020), tire rubber (Danmaliki and Saleh, 2016), mixed biowastes (Fadhil and Kareem, 2021), asphalt (Abdulhamid *et al*., 2023), and atmospheric residue (ATR) (Hasan and Fadhil, 2023) for DBT removal from model fuels.

However, to date, no studies have reported the synthesis of AC derived from coke produced via co-pyrolysis of atmospheric residue (ATR) with waste polymers such as polypropylene (PP), followed by chemical activation, for the purpose of DBT removal. Furthermore, limited information exists regarding the isothermal and kinetic behavior of such adsorbents in ADS applications. In this context, the present study aims to: Synthesize activated coke (AC) from coke derived through the thermal co-pyrolysis of ATR and polypropylene (PP) waste, followed by chemical activation using KOH; characterize the physical and chemical properties of the synthesized AC using techniques such as XRD, nitrogen adsorption–desorption, BET surface area, FESEM, and EDX; Investigate the adsorptive performance of the AC in removing dibenzothiophene (DBT) from a model fuel solution under optimized conditions; analyze the adsorption mechanism through isotherm modeling and kinetic studies to understand the interaction behavior between DBT and the AC surface; evaluate the reusability of the AC over multiple adsorption–desorption cycles to assess its stability and practical applicability.

MATERIAL AND METHODS

Precursors and chemicals

The ATR used in the preparation of the AC was kindly provided by the Alkasik refinery, north of Iraq. At the same time, the PP waste consisted of packing bags from the cement industry, which were collected from a cement factory located north of Iraq. Chemicals, like KOH (pellets, 99%), were implemented as the activator for the preparation of AC, HCl (37.0 wt.%), and iodine (I_2, solution, 0.1 N). $Na_2S_2O_3.5H_2O$ (99.0-100,5%) was used in specifying the iodine number (IN) of the resulting samples of AC. Finally, dibenzothiophene (DBT) and n-hexane (99.0 %) were used in the preparation of the model oil used in this work. All chemicals were of analytical reagent (AR) grade and were used as received, sourced from Scharlau Chemicals, Spain.

Synthesis of AC

The raw materials utilized in the synthesis of the AC were the atmospheric residue (ATR) and polypropylene (PP) waste. Initially, the ATR and PP waste were cut into approximately 1 cm-sized pieces. Next, they were mixed and loaded into a fixed-bed stainless steel pyrolysis reactor. The reactor was externally heated using an electric furnace and equipped with a condenser to collect condensable vapors, a receiving vessel immersed in an ice bath to gather the condensed liquids, and a thermocouple to monitor the pyrolysis temperature. To ensure an inert atmosphere, nitrogen gas was purged through the system for 10 minutes prior to heating. The pyrolysis process was then carried out at 400°C for 75 minutes, resulting in a solid residue (coke) that served as the precursor for the subsequent activation process. The obtained coke was first pulverized and sieved to obtain particles of 60 mesh size.

For the preparation of activated coke, 5.0 g of the sieved coke was immersed in aqueous KOH solutions at varying mass ratios (KOH: coke = 0.5:1 to 2.5:1). To ensure thorough impregnation, the KOH–coke mixtures were stirred at 250 rpm for 5h and then allowed to stand for 24h. The impregnated samples were then dried in an oven at 105 °C for 5h. The thermal activation was conducted in a muffle furnace at varying temperatures (550–850 °C) and activation times (0.5–2.0 h) with a constant heating rate of 10 °C/min. After activation, the AC samples were allowed to cool to room temperature and subsequently treated with 0.1 M hydrochloric acid to neutralize any residual KOH. The samples were then repeatedly rinsed with hot distilled water until the pH of the washings was neutral. Finally, the washed AC samples were dried at 105 °C for 10 h and stored in sealed containers for further characterization and application (G. Li *et al*., 2016) [14]. Quantification output of the resulting AC was carried out as follows:

$$\text{Yield of AC (\%)} = \frac{\text{Mass of the resultant AC (g)}}{\text{Mass of coke utilized (g)}} \text{ X } 100 \ldots\ldots\ldots\ldots\ldots\ldots\ldots (1)$$

Identification of the AC

The specific surface area, pore volume, and pore diameter of the resulting activated coke (AC) were determined based on nitrogen (N_2) adsorption–desorption isotherms measured at 77 K using a BELSORP MINI II surface area and porosity analyzer (Japan). The Brunauer–Emmett–Teller (BET) method was applied to quantify the specific surface area of the synthesized AC. Prior to measurement, the sample was degassed at 120 °C for 6h to remove any adsorbed impurities. The crystalline phases of the prepared AC were characterized using powder X-ray diffraction (XRD) with a Malvern Panalytical diffractometer (UK). The surface morphology was investigated by field-emission scanning electron microscopy (FESEM) using a TESCAN Mira instrument (Czech Republic). Elemental composition analysis of the AC was conducted using energy-dispersive X-ray spectroscopy (EDX) with an Oxford Instruments system (UK). Finally, the iodine number (IN) of the produced samples was determined following the GB/T 12496.8-2015 standard method (Zhang *et al*., 2022)

The ADS runs of DBT over the AC

The S-containing model oil (DBT in n-hexane, 500 mg/L) used in this study was prepared by dissolving DBT in n-hexane. From this model, additional working solutions (10-100 mg/L) were created to prepare a calibration plot with a correlation coefficient (R^2) of 0.9992, after measuring the absorbance of the generated DBT solutions at the maximum wavelength (325 nm) (Moosavi *et al*., 2012). Assessing the ADS effectiveness of the as-created AC to the ADS of DBT from model oil in a batch mode, 25 mL of the sulfurized fuel was mixed with a predefined amount of the AC in a 100 mL conical flask, connected to a condenser to prevent n-hexane loss by evaporation. The AC-sulfurized fuel mixture was shaken at 250 rpm on a heater-stirrer fitted with an adjustable temperature controller. After the ADS process, the AC particles were stripped from the sulfurized model through centrifugation at 5000 rpm for 5 minutes, followed by the quantification of the remaining DBT in the

sulfurized fuel at equilibrium by measuring its absorbance at 325 nm (Moosavi *et al.*, 2012). The absorbance of each sample was measured twice, and the reported value was the mean ± SD.

Determining the ADS% of the AC besides its adsorptive capacity (q_e, mg/g) was made, as per Eq.(2) and Eq.(3), respectively.

$$ADS\ (\%) = \frac{(C_0\text{-}Ce)}{C_0} * 100 \qquad \ldots\ldots\ldots\ldots\ldots\ldots\ldots\ldots (2)$$

$$q_e = \frac{(C0\text{-}Ce)}{C_0} * 100 \qquad \ldots\ldots\ldots\ldots\ldots\ldots\ldots\ldots (3)$$

where, C_o and C_e demonstrate, respectively, the initial and equilibrium concentrations of DBT, whilst V (L) and W (g) refer, respectively, to the volume of DBT and amount of the AC used in the adsorption runs.

RESULTS AND DISCUSSION

Optimization of AC preparation

The output of coke produced by the thermal decomposition of mixed ATR-PP waste at 400 °C for 75 minutes and a heating speed of 10 °C/min amounted to 20.0 wt.%. As mentioned previously, the KOH-activation approach was followed in synthesizing the AC from this coke via the optimized procedure, as presented in Fig. (1: a, b, and c).

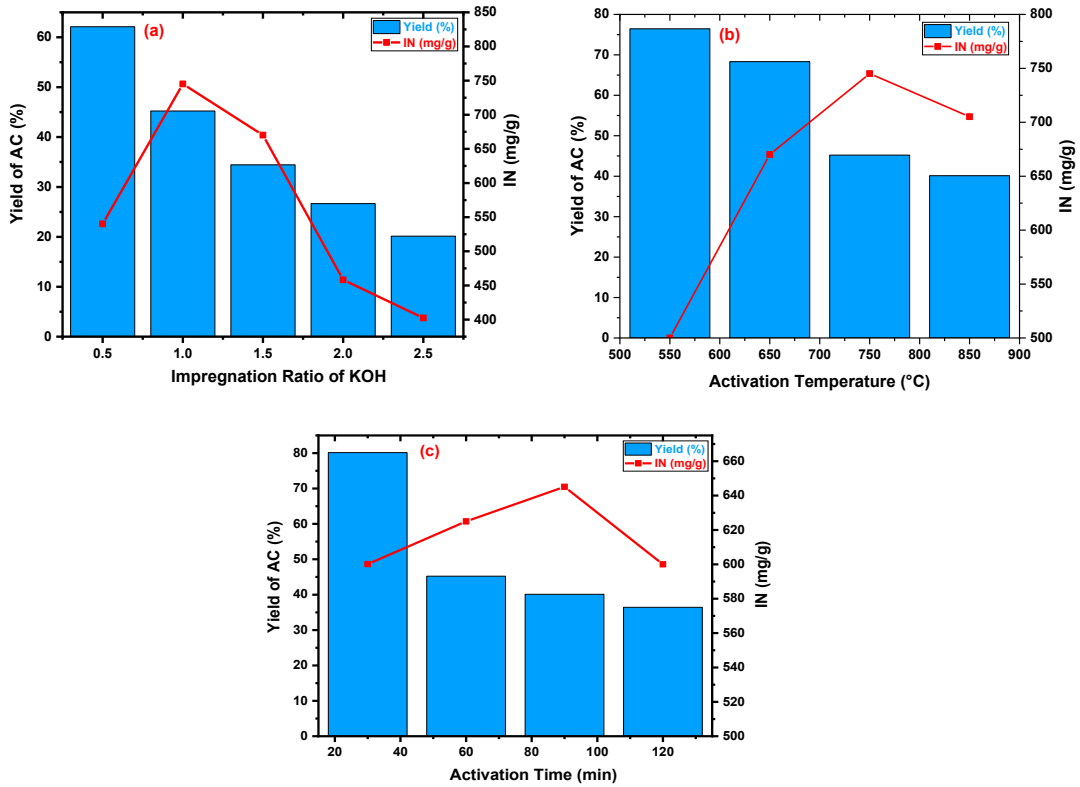

Fig. 1 (a, b, and c): Effect of the activation conditions on the output and IN of the resulting AC.

It is well known that the amount of the activator included in the chemical activation plays a potential role in the AC output and porosity. It is evident from Fig. 1(a) that the production of the AC declined with the utilization of more amount of the activator (KOH), probably attributable to the extensive diffusion of KOH into the coke matrix (Li *et al*,2017), leading to a reduction in the C-content of native coke in the form of CO, CO_2, and CH_4. Consequently, the output of the resultant AC decreased (Wang and Liang, 2020). Conversely, it was observed that increasing the KOH amount from 0.5:1 to 1:1 enhanced the porosity of the produced AC, as measured by the IN. This conclusion pertains to the formation of a novel porous structure in the resultant AC, arising from the generation of gases and other substances from the C-skeleton of coke due to the influence of KOH. However, KOH concentrations above 1:1 reduced the IN of the resultant AC, presumably due to the conversion of micropores within the AC structure into larger pores, resulting from the collapse of the walls that separate the micropores (Li *et al*.,; Wang and Liang, 2020).

Ascending the temperature of activation from 550 ˚C to 850 ˚C was accompanied by a decrease in the AC output, as demonstrated in Fig. (1: b). This result can be attributed to the additional gasification processes of the coke at elevated temperatures, in the presence of a substantial quantity of KOH, which accelerates these reactions, leading to a reduction in the AC yield (Kumar *et al*., 2022). Conversely, raising the activation temperature from 550 ˚C to 750 ˚C was associated with an enhancement in the IN of the resulting AC samples. This outcome is most likely attributable to the fact that the increase in temperature, in conjunction with the existence of an adequate quantity of KOH, boosts the gasification reactions of the pritine coke, resulting in the formation of a more developed porous structure. Despite this, raising temperatures to >750 °C resulted in a decrease in the IN. This was due to the growth of micropores into bigger pores, which was induced by the deterioration of the micropore partition walls, which ultimately resulted in a decrease in the IN (Patra,*et al* 2021) .

The effect of the activation which demonstrates period on the output and IN of the resultant AC is illustrated in Fig. (1: c), that increasing the activation period resulted in a decrease in the AC output. This reduction in the AC output occurred as a consequence of the harsh decomposition of virgin coke that occurred at high temperatures, as well as the presence of a significant quantity of KOH (Kumar *et al* ,2022) . The IN of the resultant AC, on the other hand, was enhanced as the period of activation prolonged from 30 to 60 minutes. Nevertheless, activating the samples for periods beyond 60 minutes resulted in a decrease in the IN. This was most likely caused by the disintegration of the generated microporous composition of the developed AC into broader porous ones(Patra,*et al* 2021).

Identification of the ideal AC

The activated coke (AC) prepared through the chemical activation of coke obtained via the thermal carbonization of a mixture of ATR and polypropylene (PP) waste at 750 °C for 1 h, using a 1:1 KOH-to-coke impregnation ratio and a heating rate of 10 °C/min, was identified as the optimal sample. Accordingly, this sample was subjected to detailed characterization using multiple analytical techniques to evaluate its crystalline structure, morphology, and textural properties. The N_2 adsorption–desorption isotherms Fig. (2: a) were used to determine the specific surface area, average pore diameter, and total pore volume of the synthesized AC. The isotherm exhibited Type IV behavior with an H4 hysteresis loop, indicating the presence of a mixed microporous–mesoporous structure (da Silva *et al*., 2022). The BET specific surface area (SA_{BET}) of the AC was found to be 220.96 m²/g, with an average pore diameter of 2.95 nm, confirming its mesoporous nature (Figure 2b).

Additionally, the BJH surface area was measured at 45.60 m²/g. From the comparison of the SA_{BET} and BJH values, it was estimated that micropores accounted for approximately 79.36% of the total surface area, whereas mesopores contributed 20.64%. These results confirm that the prepared AC possesses a hierarchical pore structure comprising both micro- and mesopores.

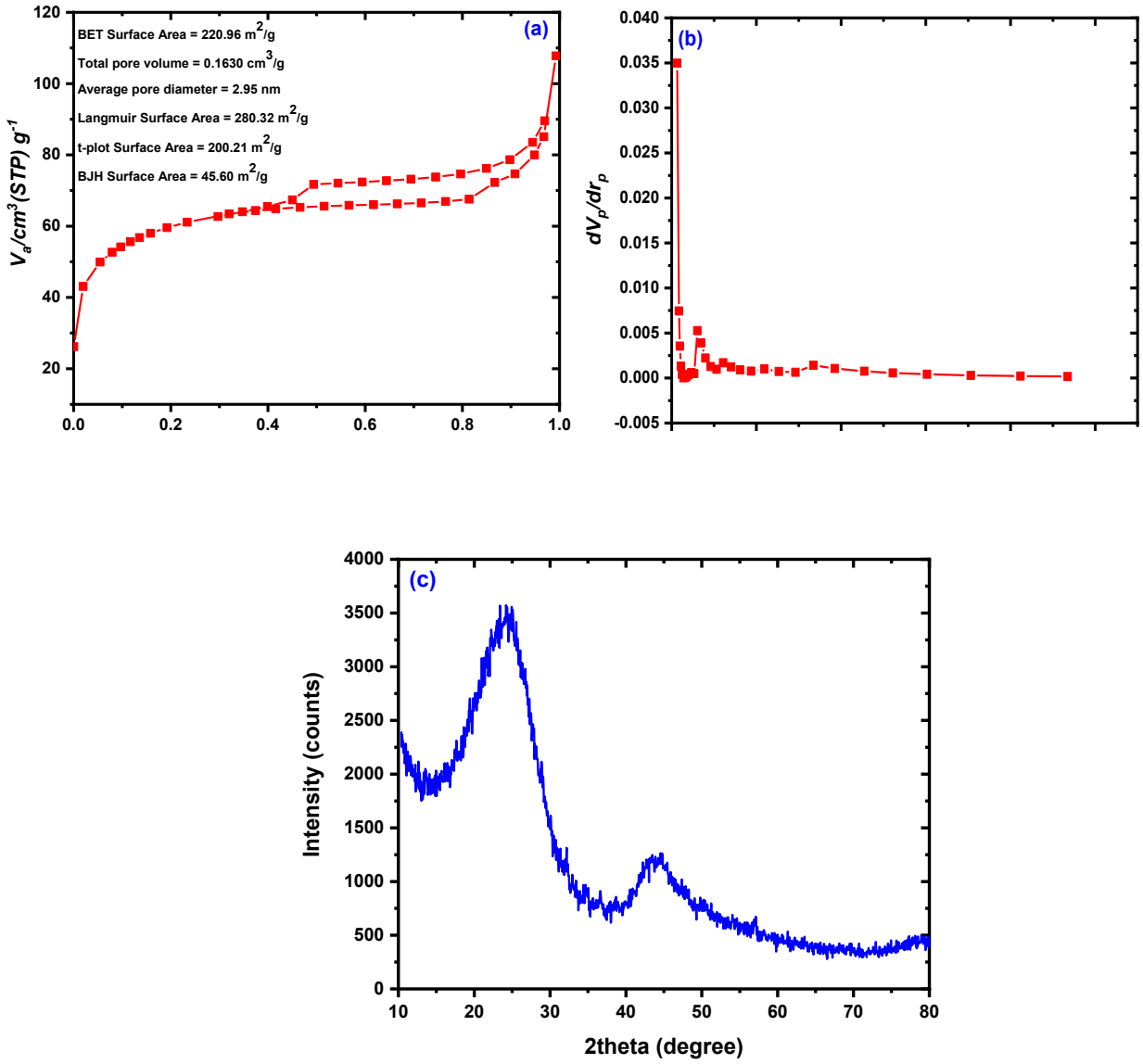

Fig. 2(a, b and c): The adsorption-desorption isotherms of N_2 gas and XRD patterns of the produced AC.

Following Fig. (2: c), the XRD patterns of the as-created AC showed two wide, distinct peaks, the first was noticed at 2θ = 26°, while the second was found at 2θ =43°. These bands correspond to the diffraction planes (002) and (100), respectively, suggesting that the structure of the produced AC is primarily amorphous (Kumari *et al*., 2022).

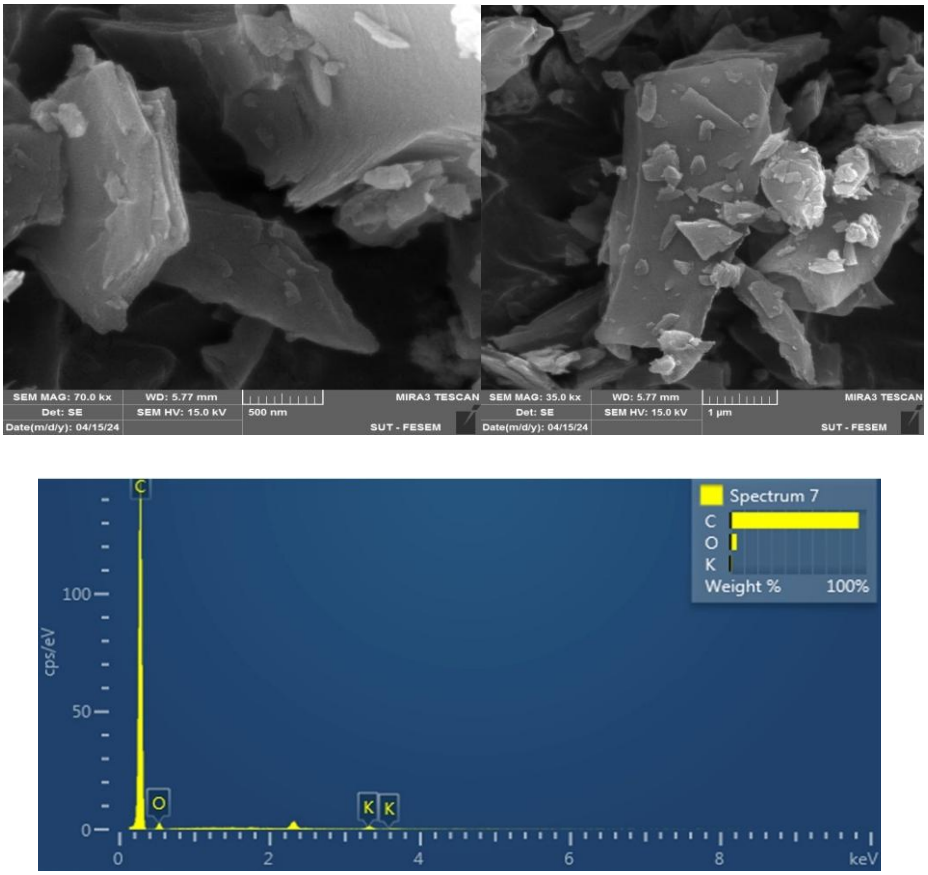

Fig. (3): FESEM photos and EDX mapping of the resulting AC.

The SEM photos of the resulting AC at various magnifications are displayed in Fig. (3: a). These images exposed that the AC surface was uneven and rough, with some visible grains. Additionally, it was noted that its surface had round-shaped voids, in addition to pores and cracks of various shapes and sizes. Consequently, the adsorption effectiveness increases as a result of the occurrence of these cavities and voids, which facilitate the access of adsorbate molecules to the AC pores (da Silva *et al*., 2022). The elemental analysis outcomes deduced from the EDX studies of AC revealed that C (94.08%) was the most abundant element, followed by O (4.79%) Fig. (3: b).

The elemental analysis mapping of the created AC also indicated the existence of a trace quantity of K, ensuring that KOH was completely consumed when real coke was converted into AC (Kumari *et al*,2022).

The ADS studies of DBT

The ADS of DBT was examined in relation to different sorbent dosages (0.05–0.40 g). With the increment of the adsorbent dosage, the ADS performance of DBT is enhanced, as shown in Fig. (4), since with the increment of the AC dosage, more accessible surface area and sites will be available for the effective adsorption of DBT (Nawar *et al* ,2025). The ADS% of DBT rose from 60.12% to 98.89 % when the AC mass increased from 0.05 g to 0.30 g. Increasing AC dosages beyond 0.30 g resulted in minimal ADS% of DBT owing to the aggregation of AC particles, which reduced the surface and sites available for DBT elimination (Nawar *et al* ,2025).

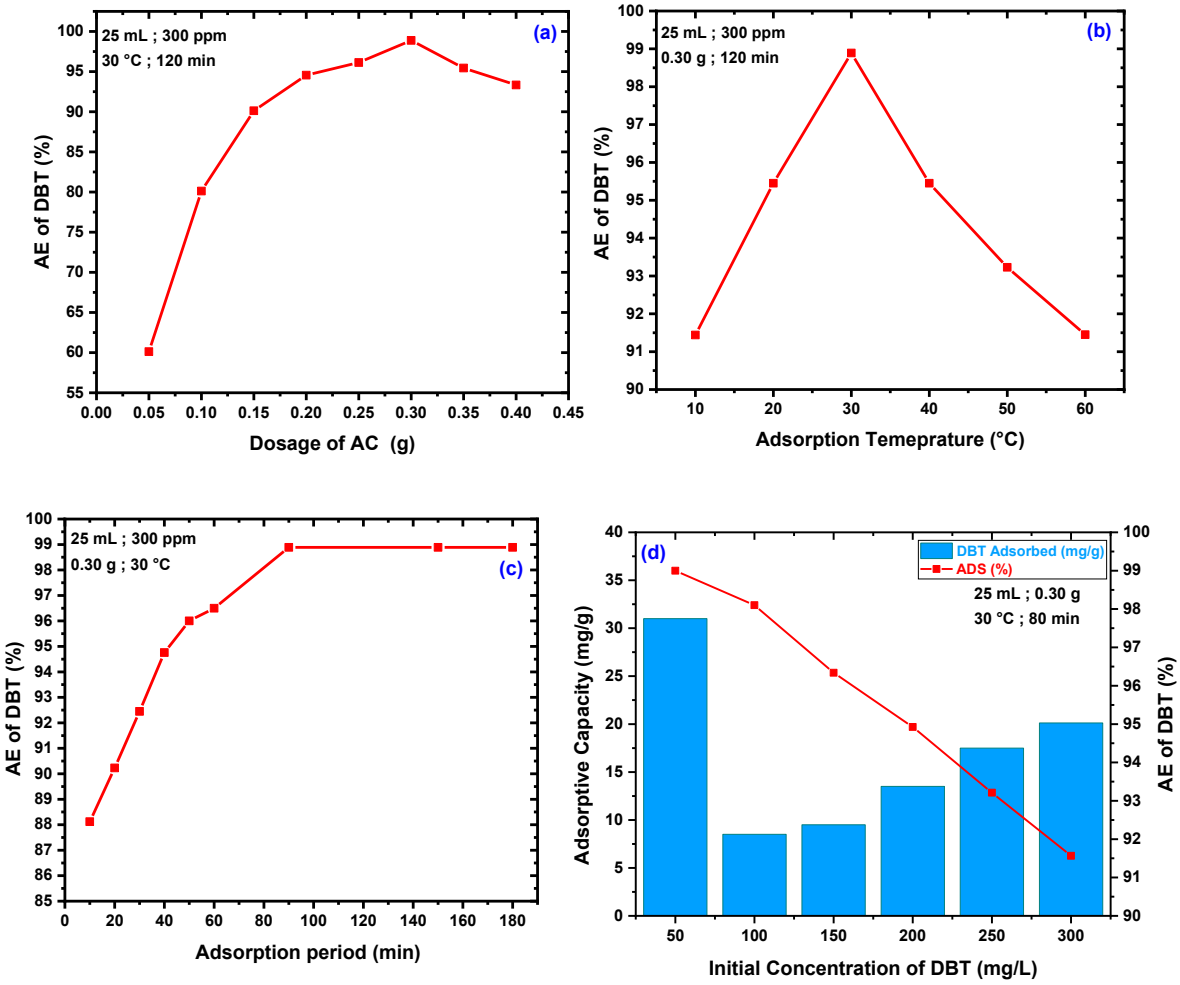

Fig. 4: Influence of variables on the AE% of DBT over the resulting AC.

The temperature effect on the ADS performance of DBT over AC was studied at 10, 20, 30, 40, 50, and 60 °C, using the conditions demonstrated in Fig. (4b). The outcomes presented in this figure indicate that the adsorption of DBT increases with temperature, suggesting that the adsorption of DBT over the as-produced AC is endothermic. The ADS% rose from 91.44% to 98.89% as the adsorption temperature increased from 10°C to 30 °C. The increase in adsorption with increasing temperature indicates that DBT removal by the AC involves both physical and chemical sorption (Fengyang *et al*., 2020). Nonetheless, temperatures above 30 ˚C decreased the ADS% of DBT, likely owing to weakened attraction forces between the DBT species and surface effective groups on the AC surface, resulting in reduced ADS performance of DBT (Abdelho *et al*. ,2005). For commercial applications, determining the time it takes to reach equilibrium is crucial. Consequently, as previously mentioned, DBT extraction by the created AC was evaluated at different intervals, ranging from 10 to 180 minutes, while maintaining the other settings constant. Rapid DBT exclusion over the as-developed AC was raised within the first five minutes of the elimination process, as shown in Fig. (4) After 30 minutes, the highest ADS was reached, and DBT deletion did not improve as a result of achieving equilibrium. These results were in line with those of other researchers (Bamufleh, 2009; Li *et al*., 2017).

As shown in Fig. (4: d), the initial DBT concentration was determined by adjusting the DBT concentration from 50 g/L to 300 mg/L while maintaining other parameters. The amount of DBT absorbed (q_e, mg/g) increased as the concentration increased. An increase in the molecular diffusion

driving force may be responsible for this result, which would enhance the interactions between the sorbate species (DBT) and the unfilled energetic sites on the AC surface (Bamufleh, 2009). When DBT was removed from several model oils using a variety of adsorbents, the results obtained were consistent with those published by previous authors (Alhamed and Bamufleh, 2009; Bamufleh, 2009).

Conversely, Fig. (4: a) demonstrates that as the original DBT concentration increased, the ADS% of DBT decreased. The specific amount of AC needed in the adsorption process represents the limited number of available adsorption sites, which is responsible for this outcome. Consequently, a large concentration of adsorbate causes considerable congestion at the adsorption sites, which reduces the effectiveness of pollutant removal (Bamufleh, 2009).

Modelling of DBT adsorption isotherms and kinetics by the AC

Practically, the isotherm equation relates the concentration of adsorbate in solution to its adsorbed quantity on the sorbent's surface at equilibrium (Mguni,2024). Two prominent mathematical models, viz. the Langmuir and the Freundlich isotherms, were employed to match the adsorption curves of DBT by the as-produced AC across a range of concentrations (50–300 mg/L) at 30 ˚C. Non-linear plots of the Langmuir isotherm (Eq. (4)) and the Freundlich isotherm (Eq. (5)) were applied to express DBT adsorption over the said AC.

$$q_e = \frac{K_L C_e}{K_L C_e} \quad \ldots\ldots\ldots\ldots\ldots\ldots (4)$$

$$q_e = K_L C_e^{1/n} \quad \ldots\ldots\ldots\ldots\ldots\ldots (5)$$

Where K_L, K_F, and n are, respectively, the Langmuir constant, contaminant adsorption capacity, and factor of homogeneity. (Table 1) presents the values associated with these constants, along with the values of the correlation coefficient (R^2). Following the R^2 values, the Freundlich isotherm was more compatible in expressing the adsorption of DBT on the said AC than the Langmuir isotherm. This outcome demonstrates a multi-layer coverage of DBT over the as-created AC surface. Additionally, it suggests that the surface of the produced AC is heterogeneous (Nayyef and Fadhil, (2023).

Table (1): Constants of the adsorption isotherms of DBT over the AC.

Langmuir isotherm			**Freundlich isotherm**		
R^2	K_L (L/g)	Q_m (mg/g)	R^2	K_F ((mg/g)/(mg/L)$^{1/n}$	n (mg/g)
0.9576	0.1308	26.37	0.9827	5.04	2.27

The kinetics studies aid in explaining the mechanism as well as the rate of sorbate adsorption by a given sorbent Nayyef and Fadhil, (2023). The most prevalent models of adsorption kinetics, namely the pseudo-1st-order (PFO), pseudo-2nd-order (PSO), and intraparticle diffusion (IPD) models, were examined to express the DBT adsorption data. The non-linear models of PFO, PSO, and IPD models adopted in describing DBT adsorption data are respectively given in Eq. (6), Eq. (7), and Eq. (8)

$$q_t = q_t\text{-}e^{-k1t} \quad \ldots\ldots\ldots\ldots\ldots\ldots (6)$$

$$q_t = \frac{k2q_e^2}{1+k2q_et} \quad \ldots\ldots\ldots\ldots\ldots\ldots (7)$$

$$q_t = K_{id}t^{0.5} + C \quad \ldots\ldots\ldots\ldots\ldots\ldots (8)$$

Where, q_t (mg/g), k_1, k_2, K_{id}, and C are respectively the amount of DBT adsorbed at a given time (min), the PFO rate constant, the PSO rate constant, the intra-particle diffusion rate constant, and a constant related to the thickness of the boundary layer. It was observed that the IPD was not suitable for expressing the adsorption of DBT by the said AC, as its curve didn't pass through the origin, indicating that it is not the only rate-determining step of DBT adsorption. (Table 2), which demonstrates the values of the kinetic constants, shows that the PSO was better expressed for DBT adsorption over the produced AC. These conclusions were based on the R^2 value, which was greater than that of the PFO. Another clue supporting this conclusion was the value of q_t (mg/g), which was higher than that obtained for the PFO. Consequently, the limiting step for DBT adsorption could be chemisorption, rather than physical diffusion (Al-Laylaa *et al*., 2024).

Table 2. Constants of the adsorption kinetics models of DBT over the AC.

PFO			PSO			IPD		
R^2	q_t (mg/g)	k_1 (L/mg)	R^2	q_t (mg/g)	k_2 (L/mg)	R_2	K_{id}	C
0.7970	10.52	0.3145	0.9923	12.69	0.1325	0.6139	1.14	4.50

3.5 The AC regeneration trials

The AC specimens included in the study were gathered for purposes of rejuvenation and recycling. The exhausted AC was placed in a Soxhlet system to take out DBT using n-hexane as the solvent. Following drying of the regenerated AC at 100 °C for 2 h, the desiccated AC was incorporated into the adsorption trials of DBT at the previously established operational conditions. This procedure was reiterated in every reusability round. Based on Figure 5, the findings revealed a minor reduction in the ADS% of DBT with an increase in reusability sessions. The ADS% was 97.62% in the initial reusability run. However, it decreased to 88.13% in the 5th run, indicating that the AC surface still possesses a sufficient number of operating positions ready to eradicate DBT.

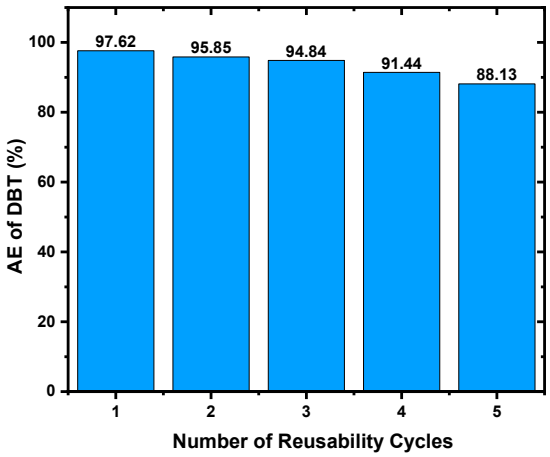

Fig. (5): Effect of reusability runs on the ADS% of the regenerated AC.

CONCLUSIONS

The study presents significant theoretical and practical implications by demonstrating that activated coke synthesized from a blend of the ATR and PP waste via co-pyrolysis and KOH activation can serve as an efficient and environmentally friendly adsorbent, particularly in desulfurization applications. The findings highlight that the optimal sample, produced at 750°C for one hour with a 1:1 KOH-to-coke ratio, exhibits a high specific surface area and a hierarchical porous structure with a dominant micro porous fraction. This mixed microporous–mesoporous architecture enhances the accessibility and diffusion of adsorbate molecules, making the material particularly effective for removing bulky organic sulfur compounds, such as DBT. The study highlights the

potential for converting industrial waste into valuable materials, thereby contributing to both sustainability and cost-effectiveness. However, several limitations exist, including that the adsorption performance was primarily evaluated for a single sulfur compound, which may not fully represent its effectiveness across a broader range of pollutants. Furthermore, further research is recommended to evaluate its performance in dynamic systems and its application at an industrial scale.

REFERENCES

Abdelho, T.; Fadel, A. B.; Al-Saffar, F.; Al-Dabouni, A., & Al-Dabouni, I. (2005). The effect of the chemical composition of asphalt and carbonization methods on the adsorptive qualities of activated carbon. *J. Mesopot. Sci*., **16**(7), 45–56. Doi.org/10.1016/j.ibiod.2016.05.003.

Abdulhamid, Q.M.; Al-Tikrity, E.T.; Fadhil, A.B.; Foot, P.J. (2023) Thermal Cracking of Al-Dora Asphalt for the Simultaneous Production of Light Fuel and Activated Carbon for Desulfurization Process. *J. Anal. Appl. Pyrolysis* **173**, 106072.

Alhamed, Y. A.; Bamufleh, H. S. (2009). Sulfur removal from model diesel fuel using granular activated carbon from dates' stones activated by $ZnCl_2$. *Fuel*, **88**(1), 87–94. Doi.org/10.1016/j.fuel.2008.07.019

Al-Laylaa, N. M. T.; Yahyab,O.M.; Altamerc,M.H.; Fadhil, A. B. (2024). Kinetic and isothermal investigation on the excellent adsorption removal of dibenzothiophene from model fuel over MnO/activated carbon composite. *Rus. J. Gen. Chem*., **94**(4), 922–934. Doi.org/10.1134/S1070363224601128.

Bamufleh, H. S. (2009). Single and binary sulfur removal components from model diesel fuel using granular activated carbon from dates' stones activated by $ZnCl_2$. *Appl. Catal. A: Gen.*, **365**(2), 153–158. Doi.org/10.1016/j.apcata.2009.06.005

Chen, Y.; Tian, Q.; Tian, Y.; Cui, J.; and Wang, G. (2021). Ultra-deep oxidative desulfurization of fuel with H_2O_2 catalyzed by mesoporous silica-supported molybdenum oxide modified by Ce. *Appl. Sci*., **11**(5), 2018. Doi.org/10.3390/app11052018

da Silva, M. C.; Schnorr, C.; Lütke, S. F.; Knani, S.; Nascimento, V. X.; Lima, É. C. ; Dotto, G. L. (2022). KOH activated carbons from Brazil nut shell: Preparation, characterization, and their application in phenol adsorption. *Chem. Engin. Rese. Design*, **187**, 387-396 . Doi.org/10.1016/j.cherd.2022.09.026.

Danmaliki, G.I.; Saleh, T. A. (2016). Influence of conversion parameters of waste tires to activated carbon on adsorption of dibenzothiophene from model fuels. Journal of Cleaner Production, **117**, 50-55. Doi.org/10.1016/j.jclepro.2016.01.073.

Debouni, A.; Debouni, I. (2005). Purification of raw mishoral sulfur from hydrocarbon impurities with heat treatment compared between industrial transportation methods. *J. Mesopotamia Sci.*, **16**(7), 80-87.

Fadhil, A. B.; Saeed, H. N; Saeed, L. I. (2020). Polyethylene terephthalate waste-derived activated carbon for adsorptive desulfurization of dibenzothiophene from model gasoline: Kinetics and isotherms evaluation. *Asia-Pacific J. Chem. Engin*. e2594. Doi.org/10.1002/apj.2594.

Fadhil, A. B.; Kareem, B. A., (2021). Co-pyrolysis of mixed date pits and olive stones: Identification of bio-oil and the production of activated carbon from bio-char. *J. Analyt. Appl. Pyrol.*, **158**, 105249. Doi.org/10.1016/j.jaap.2021.105249.

Hasan, R.A.; Fadhil, A. B. (2023). Conversion of atmospheric residue into upgraded fuel and carbon adsorbent for the adsorptive desulfurization process, Fullerenes, Nanotubes Carbon Nanostruct. **31**(5) 423–434. Doi.org/10.1016/j.ibiod.2016.05.003.

Hussein, A.A.; Fadhil, A.B. (2021). Kinetics and isothermal evaluations of adsorptive desulfurization of dibenzothiophene over mixed bio-wastes derived activated carbon. *Energy Sources, Part A: Recovery, Utiliz. Envir. Effects*, **1**(20), 5357–5376. Doi.org/10.1080/15567036.2021.1895372.

Kumar, D. P.; Ramesh, D.; Subramanian, P.; Karthikeyan, S., Surendrakumar, A. (2022). Activated carbon production from coconut leaflets through chemical activation: Process optimization using Taguchi approach. *Biores. Techn. Reports*, **19**, 101155. Doi.org/10.1016/j.biteb.2022.101155.

Kumari, M., Chaudhary, G. R., Chaudhary, S., & Umar, A. (2022). Transformation of solid waste into activated carbon for wastewater treatment: A review. *Coll. Surfaces A: Physicoch. Engin. Aspects*, **647**, 129041. Doi.org/10.1016/j.colsurfa.2022.129041

Kumari, M.; Chaudhary, G. R.; Chaudhary, S., and Umar, A. (2022). Transformation of solid plastic waste to activated carbon fibres for wastewater treatment. *Chem.*, **294**, 133692. Doi.org/10.1016/j.chemosphere.2022.133692.

Li, G.; Li, J.; Tan, W.; Jin, H.; Yang, H.; Peng, J.; Barrow, C. J.; Yang, M.; Wang, H., Yang, W. (2016). Preparation and characterization of the hydrogen storage activated carbon from coffee shell by microwave irradiation and KOH activation. *Intern. Biodet. Biodegr*., **113**, 386–390. Doi.org/10.1016/j.ibiod.2016.05.003 .

Lv, H.; Cui, L.; Xu, X.; Cen, L.; Xu, J.; Cao, F. (2022). Investigation on aquathermolysis desulfurization by cutting off C–S bond in thiophene over Fe–Zr–Al catalyst facilitated by surfactants. *Energy Sources, Part A: Rec. Utiliz. Envir. Effects*, **44**, 5755–5765. Doi.org/10.1080/15567036.2022.2087805(

Mguni, L. L.; Nkomzwayo, T.; Yao, Y. (2024). Effect of support and NiO loading on adsorptive desulfurization of diesel fuel. *Separ. Sci. Techn*., **59**(1), 122–137. Doi.org/10.1080/01496395.2024.2315616

Moosavi, E. S.; Dastgheib, S. A., Karimzadeh, R. (2012). Adsorption of theophanic compounds from model diesel fuel using copper and nickel impregnated activated carbons. *Energies*, **5**(10), 4233–4250. Doi.org/10.3390/en5104233.

Moreira, H. L.; Brandão, F. V.; Hackbarth, D.; Maass, A. M.; Ulson de Souza, A. A.; Guelli U. de Souza, S. M. A. (2017). Adsorptive desulfurization of heavy naphthenic oil: Equilibrium and kinetic studies. Chem. Engin. Sci., **172**, 1–23. Doi.org/10.1016/j.ces.2017.06.020

Nayyef, A. W.; Fadhil, A. B. (2023). Elimination of dibenzothiophene from model gasoline by binary biowastes-derived activated carbon. *Chem. Engin. Techn*., **46**(4), 681-693. Doi.org/10.1002/ceat.202200502.

Patra, B. R.; Nanda, S.; Dalai, A. K.; Meda, V. (2021). Taguchi-based process optimization for activation of agro-food waste biochar and performance test for dye adsorption. *Chem.*, **285**, 131531. Doi.org/10.1016/j.chemosphere.2021.131531.

Saha, B.; Vedachalam, S., and Dalai, A. K. (2021). Review on recent advances in adsorptive desulfurization. *Fuel Proc. Techn*., **214**, 106685. Doi.org/10.1016/j.fuproc.2020.106685

Wang, J.; Lei, S.; Liang, L. (2020). Preparation of porous activated carbon from semi-coke by high temperature activation with KOH for the high-efficiency adsorption of aqueous tetracycline. *Appl. Surface Sci*., **530**, 147187. doi.org/10.1016/j.apsusc.2020.147187.

Xiong, F.; Rother, G.; Tomasko, D.; Pang, W.; Moortgat, J. (2020). On the pressure and temperature dependence of adsorption densities and other thermodynamic properties in gas shales. *Chem. Engin. J.*, **395**, 124989. Doi.org/10.1016/j.cej.2020.124989.

Yaqoob, N. H.; Naife, T. M.; Shareef, Z. N. (2025). Adsorptive desulfurization of benzothiophene from simulated fuelusing Ni/ Γ-Al_2O_3 as an adsorbent; performance, adsorption, andkinetic study. *Iraqi J. Chem. Petrol. Engin*., **26**(1), 89 – 97.

Zhang, G.; Yang, H.; Jiang, M.; Zhang, Q. (2022). Preparation and characterization of activated carbon derived from deashing coal slime with ZnCl2 activation, Colloids Surfaces a Physicochemist. *Eng. Asp*. **641**, 128124. Doi.org/10.1016/j.colsurfa.2022.128124

تحضير الكاربون المنشط من خلال الكربنة المشتركة لمخلفات التقطير الجوي ومخلفات البولي بروبيلين وتنشيطه بهيدروكسيد البوتاسيوم لإزالة الكبريت من الوقود النموذجي

منتهى حيدر يعقوب **عبد الرحمن باسل فاضل**

قسم الكيمياء/ كلية العلوم/ جامعة الموصل

الملخص

تزايد الحاجة إلى طرق صديقة للبيئة لتقليل محتوى الكبريت في وقود النقل دفع إلى البحث عن مواد ماصة فعالة ومنخفضة التكلفة. تهدف هذه الدراسة إلى تصنيع فحم منشط جديد (AC) من مزيج من البقايا الجوية (AR) من مصفى القيّارة وبقايا البولي بروبيلين (PP) المجمعة من مصنع إسمنت. تم تنفيذ عملية التشارك في الكربنة عند درجة حرارة 400 درجة مئوية لمدة ساعة واحدة، تلتها عملية تنشيط كيميائي باستخدام هيدروكسيد البوتاسيوم(KOH) .

تم توصيف الفحم المنشط الناتج باستخدام حيود الأشعة السينية(XRD) ، وقياسات الامتزاز والانفراج للنيتروجين عند 77 كلفن، ومجهر المسح الإلكتروني الباعث للمجال(FESEM) ، ومطيافية الأشعة السينية المشتتة للطاقة (EDX) لتقييم البلورية، والمساحة السطحية، وبنية المسام، والتشكل، والتركيب العنصري. أظهر الفحم المنشط المحسّن مساحة سطحية قدرها 220.96 متر مربع/غرام ومتوسط عرض مسام قدره 2.95 نانومتر، مما يشير إلى بنية مسامية متوسطة (ميسوبور) .

تم اختبار أداء الامتصاص للفحم المنشط باستخدام وقود نموذجي يحتوي على ثنائي بنزوثيوفين (DBT) مذاب في الهكسان. وقد تم تحقيق كفاءة إزالة بلغت 97.62٪ تحت الظروف المثلى (0.3 غرام من الفحم المنشط عند درجة حرارة 30 درجة مئوية لمدة 80 دقيقة). وتبعَت عملية الامتزاز نموذج إيزوثرم فريندلخ وحركية من الدرجة الثانية الكاذبة. علاوة على ذلك، أظهر الفحم المنشط قابلية جيدة لإعادة الاستخدام، حيث احتفظ بكفاءة إزالة قدرها 88.13٪ بعد خمس دورات تجديد.

تُظهر الدراسة أن الفحم المنشط المُصنّع هو مادة ماصة واعدة وفعالة لإزالة الكبريت من وقود النقل، ويُقدم حلاً مستدامًا من خلال الاستفادة من النفايات الصناعية.

الكلمات المفتاحية: التفحيم المشترك، مخلفات التقطير الجوي، مخلفات البولي بروبلين ، ازالة ثنائي بنزو ثايوفين